

Correlation between the surface conductivity and structure of SnO₂(110)

This article has been downloaded from IOPscience. Please scroll down to see the full text article.

1991 J. Phys.: Condens. Matter 3 S291

(<http://iopscience.iop.org/0953-8984/3/S/046>)

View [the table of contents for this issue](#), or go to the [journal homepage](#) for more

Download details:

IP Address: 129.252.86.83

The article was downloaded on 27/05/2010 at 11:25

Please note that [terms and conditions apply](#).

Correlation between the surface conductivity and structure of SnO₂(110)

G L Shen†‡, R Casanova†¶, G Thornton† and I Colera‡

† Interdisciplinary Research Centre in Surface Science and Chemistry Department, Manchester University, Manchester M13 9PL, UK

‡ Laboratorio de Física de Superficies, Instituto de Ciencia de Materiales, CSIC, Serrano 144, 28006 Madrid, Spain

Received 25 April 1991

Abstract. XPS, UPS, work function, surface conductivity and LEED measurements of SnO₂(110) have been performed with the purpose of exploring the effect of annealing the clean, amorphous surface in the temperature range $300 \leq T \leq 1100$ K. Most of the results are consistent with earlier work. However, the extended temperature range employed allows the presence of the 1×2 high-temperature phase to be confirmed. The measurements point to a missing bridging-O row model for this phase.

1. Introduction

Rutile SnO₂ surfaces, particularly the lowest-energy, (110) face, have received wide attention [1-7]. This largely derives from the use of the material in gas-sensing and other applications. Most of the applications rely on the O-vacancy-derived n-type semiconductor behaviour of the 3.6 eV bandgap material. Gas-sensing relies on the conductivity increase (decrease) in reducing (oxidizing) gases and the research has sought a more complete understanding of the basic operating mechanism with an aim of improving performance. This includes attempts to relate conductivity information to the surface structure and stoichiometry of SnO₂(110)[1-6]. In this paper we focus on *in-situ* measurements of the surface conductivity and composition. We extend the range of earlier measurements and investigate discrepancies in the reported surface structures. This allows us to suggest a structure for the ordered-defect SnO₂(110) 1×2 phase.

2. Experimental details

LEED, Auger electron spectroscopy (AES) and He I ($h\nu = 21.22$ eV) photoemission experiments were performed using an instrument described elsewhere [8]. A Mg K α ($h\nu = 1253.6$ eV) x-ray photoemission spectroscopy (XPS) source, mass spectrometer

‡ Permanent address: Institute of Electronics, Academia Sinica, PO Box 2652, Beijing 100080, People's Republic of China.

¶ Permanent address: Universidad de los Andes, Facultad de Ciencias, Departamento de Física, Laboratorio de Física de Superficies, Mérida-Estado, Mérida, Venezuela.

and surface conductivity probe have been added to this instrument. In this work He I photoemission spectra were recorded with a photoemission energy resolution of 0.1 eV (FWHM) and an angular resolution of $\pm 2^\circ$. Photoemission spectra are referenced to the Fermi level, E_F , recorded from the Ta sample holder. Sheet conductance measurements employed an *in situ* four-point resistivity probe (Jandel Engineering Ltd) similar to that described in [1]. The base pressure of the instrument during measurements was 1×10^{-10} mbar.

The $\text{SnO}_2(110)$ sample (10 mm \times 3 mm \times 2 mm) was mechanically polished to within 1° of the (110) plane. The sample was cleaned *in situ* by 500 eV Ar^+ -bombardment (3 μA) for 5 min.

3. Results and discussion

The LEED patterns obtained following annealing of the Ar^+ -bombarded $\text{SnO}_2(110)$ surface are shown in figure 1. Three different well-defined LEED patterns were observed depending on the period of the anneal and the temperature employed. Typically, annealing at 900 K results in a 4×1 pattern, followed by 1×1 after further annealing at 1000 K and a 1×2 pattern on raising the anneal temperature to 1100 K. In addition, a diffuse 1×1 LEED pattern was observed after annealing in the range 400–840 K, with some 4×1 character introduced at the high temperature end of the range. These observations are similar to those reported by De Frésart *et al* [6], with the exception that we do not observe a centred beam associated with the 4×1 pattern. This difference also applies to the observations of Cox *et al* [2], who report a $c(2 \times 2)$ pattern following an 800 K anneal. In addition, these authors only observed a 1×2 pattern after extensive Ar^+ -bombardment and annealing [2]. The latter difference could well arise from a difference in sample history, since Cox *et al* [2, 3] employ a much more extensive oxidation treatment (~ 1 mbar at 700 K) than that used by De Frésart *et al* [6] or in this work. As yet we do not have an explanation for the discrepancies associated with the centred phases.

The corresponding changes to the O 1s/Sn 3d XPS ratio, work function and sheet conductivity are shown in figure 2. The XPS ratio is not modified until the anneal temperature reaches a temperature of about 900 K, corresponding to the formation of the well-defined surface phases. At higher anneal temperatures the XPS ratio increases. The work function decreases on annealing the Ar^+ -bombarded surface, reaching a minimum at an anneal temperature of around 650 K. This corresponds to the appearance of diffuse LEED spots having 1×1 and 4×1 symmetry. The work function then increases with increasing anneal temperature until at 900 K it reaches a value comparable with that of the Ar^+ -bombarded surface. As for the sheet conductivity, it increases by almost four orders of magnitude over the anneal temperature range 400–900 K. It then decreases when the anneal temperature is raised through the range corresponding to the formation of the 1×1 and 1×2 phases. The variation of the band-bending with anneal temperature, monitored using the valence band position with respect to E_F in the He I photoemission spectrum, follows the same trend as the work function. It displays an increasingly downward band-bending towards the surface as the anneal temperature is increased to about 700 K. At higher anneal temperatures the downward band-bending decreases up to 1050 K. These results are qualitatively consistent with those obtained in earlier work [1–6], although in this work the anneal-temperature range is extended.

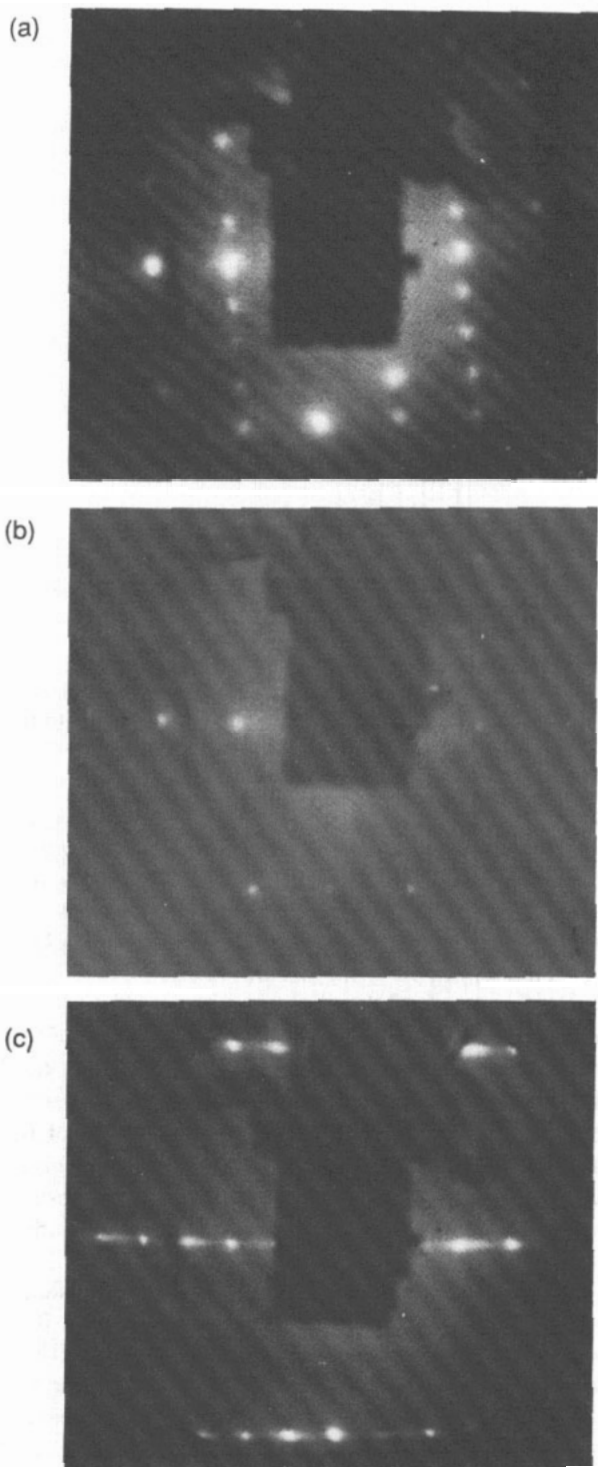


Figure 1. $\text{SnO}_2(110)$ LEED patterns recorded at room temperature and an electron energy of 68 eV obtained after sequential 10 min anneals to: (a) 900 K (4×1); (b) 1000 K (1×1) and (c) 1100 K (1×2). The horizontal axis is parallel to [011].

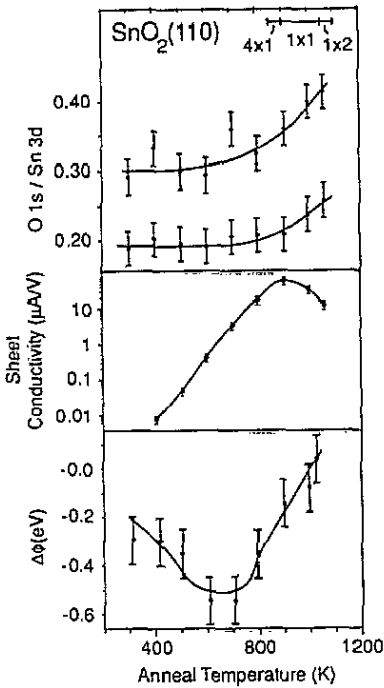


Figure 2. O 1s/Sn 3d XPS peak area ratio, sheet conductivity and work function, $\Delta\phi$, obtained at room temperature after sequential 10 min anneals to the temperatures indicated. The corresponding temperature range of surface phases is indicated.

The increase in the O 1s/Sn 3d XPS ratio with anneal temperature can be understood as a progressive re-oxidation of the surface by diffusion of oxygen from the bulk [2]. This follows surface reduction by Ar⁺-bombardment. Our work function and band-bending results are consistent with this conclusion. The work function increases over the range of increase of the XPS ratio as O atoms increasingly terminate the structure at the surface. This will deplete the accumulation layer associated with oxygen-vacancy-derived bandgap states and decrease the extent of band-bending.

Although the Ar⁺-bombarded surface contains a high concentration of O vacancies [7], the associated donor levels do not effectively contribute to the n-type conductivity in this amorphous surface. Introducing crystallinity by annealing gives rise to the increase in surface conductivity observed in figure 2(b) [2]. Oxidation of the surface by bulk O atoms after annealing at sufficiently high temperature will give rise to a decrease in carrier concentration, as evidenced by the band-bending results. These two competing processes give rise to the maximum observed in the conductivity at ~ 900 K.

The surface structure proposed for the 1 × 1 vacuum-annealed surface is shown in figure 3(b), in which all the top-layer oxygen atoms are missing [2, 3]. A 1 × 1 structure can be formed which is oxygen-terminated (see figure 3(a)), with the bridge sites fully occupied, but this requires annealing at 700 K in 1.32 mbar O₂ [3]. The data in figure 2 as well as the band-bending measurements point to a decrease in the number of surface oxygen vacancies in the 1 × 2 phase compared with 1 × 1. A structure which satisfies this requirement has been suggested for the 1 × 2 ordered O-vacancy phase of TiO₂(110) [9] and is shown in figure 3(c). As for the 4 × 1 structure, our data suggest that this should have a lower O-vacancy concentration than the vacuum

annealed 1×1 . This would require the removal of in-plane O atoms, or as suggested by Cox *et al* [2], a coincident SnO layer.

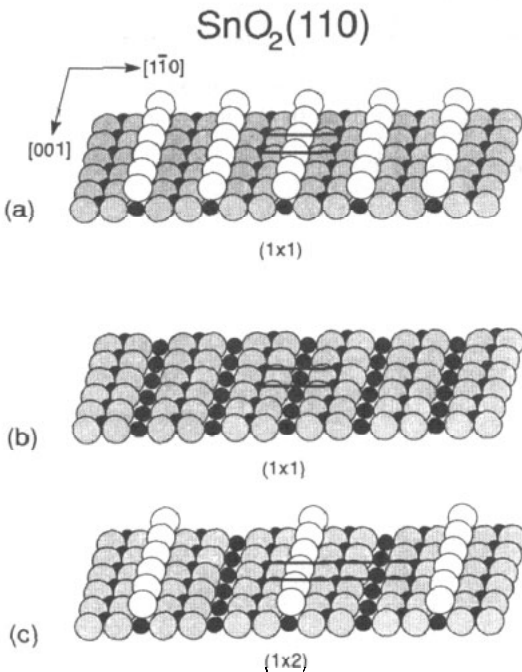


Figure 3. Structural models proposed for $\text{SnO}_2(110)$: (a) 1×1 stoichiometric surface; (b) 1×1 vacuum-annealed surface; and (c) the 1×2 structure formed by annealing to 1100 K. Open circles are the top-layer bridging oxygen atoms, and the full circles represent Sn atoms.

4. Summary

In this work we have examined the relationship between the $\text{SnO}_2(110)$ surface conductivity, work function, surface oxygen concentration and structure. By extending the temperature range we are able to confirm the presence of a 1×2 high-temperature phase. Our measurements point to a missing bridging-O row model for this phase. A discrepancy associated with centred surface phases remains.

Acknowledgments

We thank Dr R G Egdell for supplying the $\text{SnO}_2(110)$ sample. This work was funded by the SERC including the award of visiting fellowships to GLS and RC. The UK-Spanish collaboration was supported by the Program Acciones Integrades 1990-91.

References

- [1] Erickson J W and Semancik S 1987 *Surf. Sci* **187** L658

- [2] Cox D F, Fryberg T B and Semancik S 1989 *Surf. Sci.* **224** 121
- [3] Cox D F, Fryberg T B and Semancik S 1988 *Phys. Rev. B* **38** 2072
- [4] Semancik S and Cox D F 1987 *Sensors Actuators* **12** 101
- [5] Cox D F and Fryberg T B 1990 *Surf. Sci. Lett.* **227** L105
- [6] De Frésart E, Darville J and Gilles J M 1980 *Solid State Commun.* **37** 13; 1982 *Appl. Surf. Sci.* **11/12** 637
- [7] Egdell R G, Eriksen S and Flavell W R 1987 *Surf. Sci.* **192** 265
- [8] Wincott P L, Brookes N B, Law D S-L, Thornton G and King G C 1989 *J. Phys. E: Sci. Instrum.* **22** 42
- [9] Møller P J and Wu M-C 1989 *Surf. Sci.* **224** 265